Molecular Vision **1999; 5:22** <http://www.molvis.org/molvis/v5/p22>
Received 9 August 1999 | Accepted 31 August 1999 | Published 15 September 1999

Mouse fundus photography and angiography: A catalogue of normal and mutant phenotypes

Norman L. Hawes,[1] Richard S. Smith,[1,2] Bo Chang,[1] Muriel Davisson,[1] John R. Heckenlively,[3] Simon W. M. John[1,2,4]

[1]The Jackson Laboratory and [2]The Howard Hughes Medical Institute, Bar Harbor, Maine; [3]The Jules Stein Eye Institute, Los Angeles, California, and [4]The Department of Ophthalmology, Tufts University School of Medicine, Boston, Massachusetts

Purpose: Mice are an increasingly important tool in ophthalmic research. As a result of studying spontaneous and induced mutations, many new ocular diseases have been described in mice in recent years, including several degenerative retinal diseases that demonstrate progression with age. Clearly, documentation of progressive changes in clinical phenotype is an important facet of characterizing new mutations and for comparing them with human diseases. Despite these facts, there are few published photographs of mouse fundi. The small size of the mouse eye and the steep curvature of its structures have made it difficult to obtain high quality fundus photographs. The purpose of this work was to develop procedures for mouse fundus photography and angiography and to use these techniques to examine several new mouse strains with ocular abnormalities.

Methods: We have used a small animal fundus camera and condensing lens to develop a reliable technique for producing high quality fundus images of conscious albino and pigmented mice. The fundus camera also was utilized to develop a method for fluorescein angiography, which demonstrated the normal retinal vascular bed as well as abnormal vascular leakage. In addition, several mouse strains with previously unreported ocular abnormalities (including two with inherited optic nerve colobomas) and a catalogue of previously unpublished clinical images for various mutant mice are presented.

Results: Altogether, we provide clinical images for C57BL/6J, BALB/cByJ, retinal degeneration 1 (*rd1*), *Rd2*, *rd3*, *rd7*, achondroplasia, nervous, motor neuron degeneration, Purkinje cell degeneration, kidney and retinal defects, optic nerve coloboma 1, and two apparently multigenic optic nerve colobomas in a strain of mixed derivation (ONC) and the inbred CALB/Rk strain.

Conclusions: Our photography procedure reliably produces high quality images of the mouse fundus. This permitted us to record progressive retinal changes over time in the same animal, allowed us to compare the phenotypes of newly discovered retinal mutants to existing mutants at other institutions and to potentially similar human conditions, and finally, permitted us to produce a catalogue of previously unpublished clinical phenotypes for various mutant mice.

The appearance of the ocular fundus exhibits significant variation among normal individuals, different ocular diseases and different stages of a particular disease. Fundus photography is an important tool for documentation of the presence and progression of different pathologic processes. It is clear that many diseases have a genetic component and genetic studies in mice are proving valuable for learning about genes and pathologic mechanisms that contribute to disease. This is due to the powerful tools of mouse genetics, including the ability to rapidly map genes in large highly informative mouse crosses, and the ability to study gene function through gene targeting, transgenic, and random mutagenesis experiments [1-5]. Despite the strengths of mouse studies, the wealth of mutant mice with retinal disease, and the importance of clinical documentation, there are few published photographs of mouse fundi [6-10]. The difficulty in obtaining good mouse fundus photographs is primarily due to the small size of mouse eyes and the very small pupil that limits the amount of light reflected back from the fundus. A reliable system for recording high quality images of mouse retinal changes is needed. Previous reports used human fundus cameras in conjunction with a condensing lens to record features of the mouse fundus [6-10]. In our hands, however, photography with these cameras and a condensing lens was difficult and images of adequate quality were rare. Using a Kowa Genesis small animal fundus camera and a condensing lens, we have refined a procedure to reliably produce high quality color images of the fundi of conscious albino and pigmented mice. The Genesis camera is specifically designed to meet the special needs for photographing small eyes, and also allows flourescein angiography. In this report, we present our procedures for fundus photography and angiography, several new mouse strains with ocular abnormalities, and a catalogue of previously unpublished clinical phenotypes for various mutant mice, including the four retinal degeneration (rd) diseases *Pdeb*^{rd1}, *Prph2*^{Rd2}, *rd3*, and *rd7*.

Correspondence to: Simon W.M. John, Ph.D., The Howard Hughes Medical Institute, The Jackson Laboratory, 600 Main Street, Bar Harbor, ME 04609, swmj@jax.org

METHODS

Animal husbandry: All experiments were performed in compliance with the Association for Research in Visoni Ophthalmology statement for use of animals in ophthalmic and vision research. Mice were housed in cages covered with non-woven polyester filters and containing white pine bedding. The environment was kept at 21 °C with a 14 h light : 10 h dark

cycle or a 12 h light : 12 h dark cycle. The light cycles differed with mouse room and are not believed to be important for the current observations. All mice were fed NIH31 (6% fat) chow *ad libitum*, and their drinking water was acidified to pH 2.8 to 3.2 to prevent bacterial growth. The colony was monitored for specific pathogens by The Jackson Laboratory's routine surveillance program (see Jackson Laboratory Homepage, http://www.jax.org/, for specific pathogens).

Clinical examinations: To identify new phenotypes prior to fundus photography, eyes were examined with a slit lamp biomicroscope (Nikon, Tokyo, Japan) and an indirect ophthalmoscope (American Optical, Rochester, NY, USA). These instruments were used in conjunction with a 78 or 90 diopter (D) condensing lens. Pupils were dilated with a drop of 1% atropine sulfate or 1% cyclopentolate. Dilation is usually more rapid with cyclopentolate, and most mice tolerate these agents well.

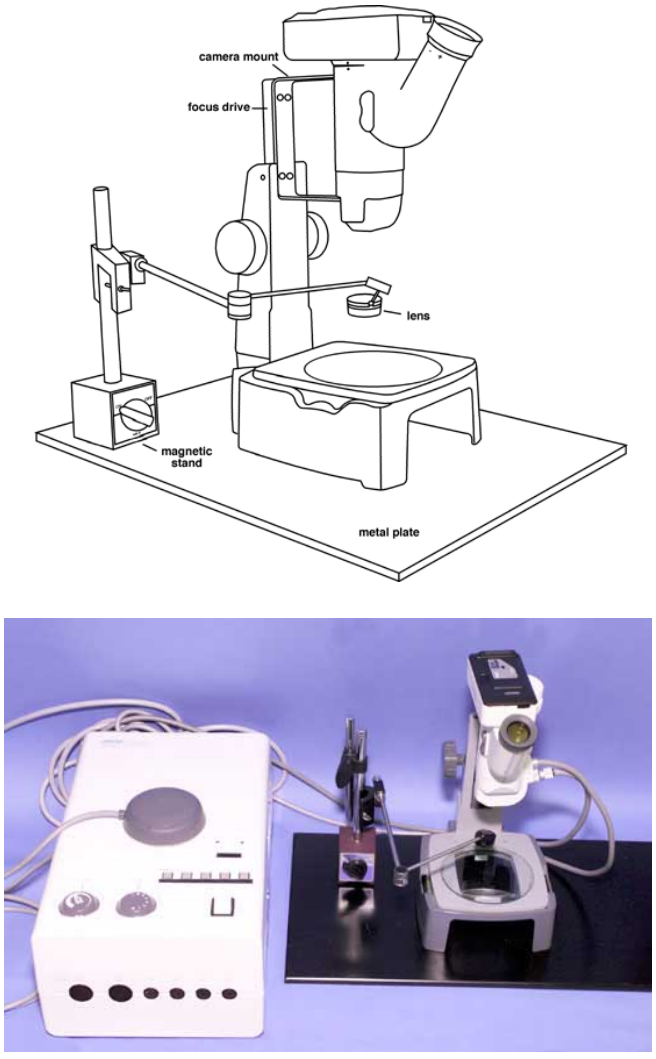

Figure 1. Diagram and photograph of fundus photography equipment. **Upper panel**: Basic features of fundus photography equipment. **Lower panel**: Photograph of actual equipment. The large white box on the left is the power supply. The foot pedal, which is normally placed on the floor, is resting on top of the power supply.

Fundus photography: A Nikon photo slit lamp (Tokyo, Japan), Kowa RC-2 human fundus camera or Kowa Genesis small animal fundus camera (Tokyo, Japan) were used to photograph mouse fundi. The instruments were used in conjunction with a condensing lens mounted between the camera and eye. The RC-2 camera was stabilized by a tripod whereas the Genesis was mounted on a modified microscope base (Figure 1, see below). Photographs were taken using conscious mice. This avoids complications of anesthesia such as clouding of the ocular media and the poor tolerance of both immature and old mice to anesthesia. The vibrissae were trimmed with fine scissors to prevent them from obscuring the photograph. If ophthalmoscopic examination did not precede fundus photography, the pupil was dilated as described above.

Our detailed procedure for the Genesis camera, which provided the best fundus images, is as follows. The camera was

TABLE 1. MOUSE INFORMATION

Common Name Or Strain	Allele Symbol	Genotype	Genetic Background	References
C57BL/6J			C57BL/6J	
BALB/cByJ			BALB/cByJ	
Retinal Degeneration 1 (*rd1*)	*Pdeb*^{rd1}	*Pdeb*$^{rd1/rd1}$	C3HeB/FeJ	12, 14, 26
Retinal Degeneration 2 (*Rd2*)	*Prph2*^{Rd2}	*Prph*$^{Rd2/Rd2}$	C3.BLiA	12, 14, 27
Retinal Degeneration 3 (*rd3*)	*rd3*	*rd3/rd3*	In(5)30Rk	12 - 15
Retinal Degeneration 7 (*rd7*)	*rd7*	*rd7/rd7*	C57BL/6J	17
Achondroplasia (cyanotic)	*cn*	*cn/cn*	STOCK a/a Tyrc/Tyrc cn+	
nervous	*nr*	*nr/nr*	C3HeB x C57BL/6J F2 not carrying *rd1*	12, 14, 19
Motor neuron degeneration	*mnd*	*mnd/mnd*	B6.KB2 congenic inbred	12, 14
Purkinje cell degeneration	*pcd*	*pcd/pcd*	C57BL/6J	12, 14, 20, 21
Kidney and retinal defects	*Krd*	*Krd/+*	C3.BLiA	12, 22
Optic nerve coloboma (ONC)		multigenic	Mixed*	
CALB/RK		multigenic	CALB/Rk**	
Optic nerve coloboma	*Onc1*	*Onc1/+*	C57BL/6J	

*First identified in a single mouse of undefined mixed background. This mouse was bred to C57BR/cdJ and the offspring intercrossed to recover the phenotype. The strain is maintained by brother-sister matings. Since this optic nerve coloboma appears to have a multigenic origin, we refer to this strain by the phenotype designator "ONC" in this paper.

** A wild derived strain caught near San Francisco and inbred by brother-sister matings.

fitted to a dissection microscope base for stability and a foot pedal (supplied with the camera) was used to operate the shutter (Figure 1). This permitted use of both hands for mouse handling. One hand was used to hold the mouse while two fingers of the other hand were used to retract the eyelids. This allows complete lid retraction with secure but gentle restraint. In rare cases, a mouse can be sedated if it cannot be held still. It was necessary to use an external condensing lens mounted 5 cm below the camera. We typically used a Volk 90D lens (Mentor, OH, USA) but 60D and 78D superfield lenses also worked well and provided different magnifications and focal depths. The lens was mounted using a Volk steady mount that is designed to attach to a slit-lamp post. The mount was attached to a post supported by a magnetic holder (Figure 1). The mouse was held on its side on the microscope platform approximately 7.5 cm beneath the lens. Focusing was achieved by moving the mouse. The use of two hands (see above) stabilizes the mouse and affords control over mouse movement, therefore, greatly facilitating focusing. The mouse position and angle were altered to study different parts of the fundus. The depth of focus was relatively shallow, so best retinal or retinal vessel focus was obtained by focusing specifically on these structures. Nevertheless, in most cases focusing to have both retina and retinal vessels in reasonable focus captured adequate detail. It was important to position the mouse to minimize reflections. Generally, this involved focusing through an off center position of the eye. Because of our interest in flourescein angiography we used the power pack that is designed for angiography. In all cases, light intensity of the visual field illuminator (used for focusing) was set high enough to see retinal details but low enough to keep the pupil from closing. The photographic flash on the powerpack has seven intensity levels and one of the two highest settings (level 6 or 7) produced best results on pigmented mice. The lower intensity (level 4) worked best for albino mice. In some cases the pupil constricted after flash photography. Photosensitivity varied primarily with strain but also with the individual mouse. The pupil constricted less frequently when atropine was used for dilation. Additionally, a second dose of atropine will sometimes allow photography after a 10 min wait. In all cases, we used Kodak Elite 200 ASA slide or print film (100 was not sensitive enough and 400 gave grainy images).

Fluorescein angiography: For retinal angiography the same general fundus photography procedure was used except that the standard camera back was replaced with one specifically manufactured to contain a barrier filter for fluorescein angiography, and the powerpack was set for angiography. Selecting this mode places the built-in exciter and barrier filters into their appropriate positions. For viewing, the eyepiece was fitted with the manufacturer-supplied barrier filter. Mice were intraperitoneally injected with 25% sodium fluorescein at a dose of 0.01 ml per 5-6 gm body weight (Akorn Inc., Decator, IL). Others have used a similar technique [11]. At injection, the timer on the power pack was engaged so that elapsed time in seconds was printed on each picture. The retinal vessels began filling about 30 s after fluorescein adminis-

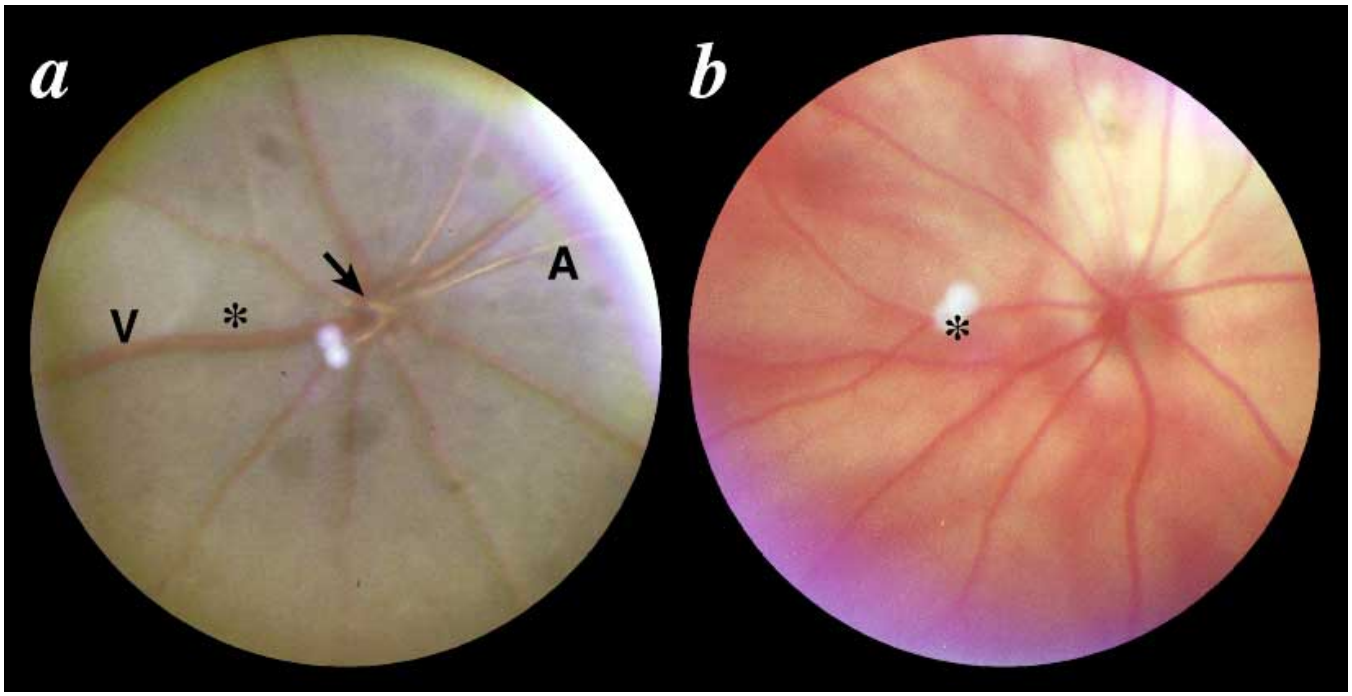

Figure 2. Normal fundi. **A**: C57BL/6J mouse, 8 weeks of age. The venules (V) are twice the diameter of the arterioles (A) and both demonstrate a clear blood column. The choroid and retina are pigmented. Focal faint patches of lighter pigmentation are evident. **B**: BALB/cByJ mouse, 12 weeks of age. Because of the absence of choroidal and retinal pigment epithelial pigmentation, the larger choroidal vessels show through the retina and the optic nerve is less well defined than in pigmented mice. Both fundi are from the right eye. The optic nerve head is indicated by an arrow and the central retina by an asterisk. For larger versions of an individual image, go to http://www.molvis.org/molvis/v5p22.

tration. Single photographs were taken at appropriate intervals. Although timing varies due to variable rates of intraperitoneal absorption, capillary washout usually occurs 5 min after dye administration. Kodak black and white Tmax 400 ASA professional film or Elite 2, 200 ASA color slide film was used.

Genetic background and genotypes: Relevant genetic information about the strains analyzed and a partial list of references pertaining to previous histologic or electroretinographic studies are provided in Table 1.

RESULTS

After experimenting with various condensing lenses in conjunction with a slit-lamp, a human fundus camera or the Kowa Genesis small animal fundus camera, we found that the Genesis produced consistently high quality images that, in our hands, are superior to those obtained with the other systems. Observations with many strains of mice have demonstrated that while cyclopentolate is ideal for clinical examination, 1% atropine provides more stable pupillary dilation that is more resistant to the bright flash lamp. For optimal dilation, drops

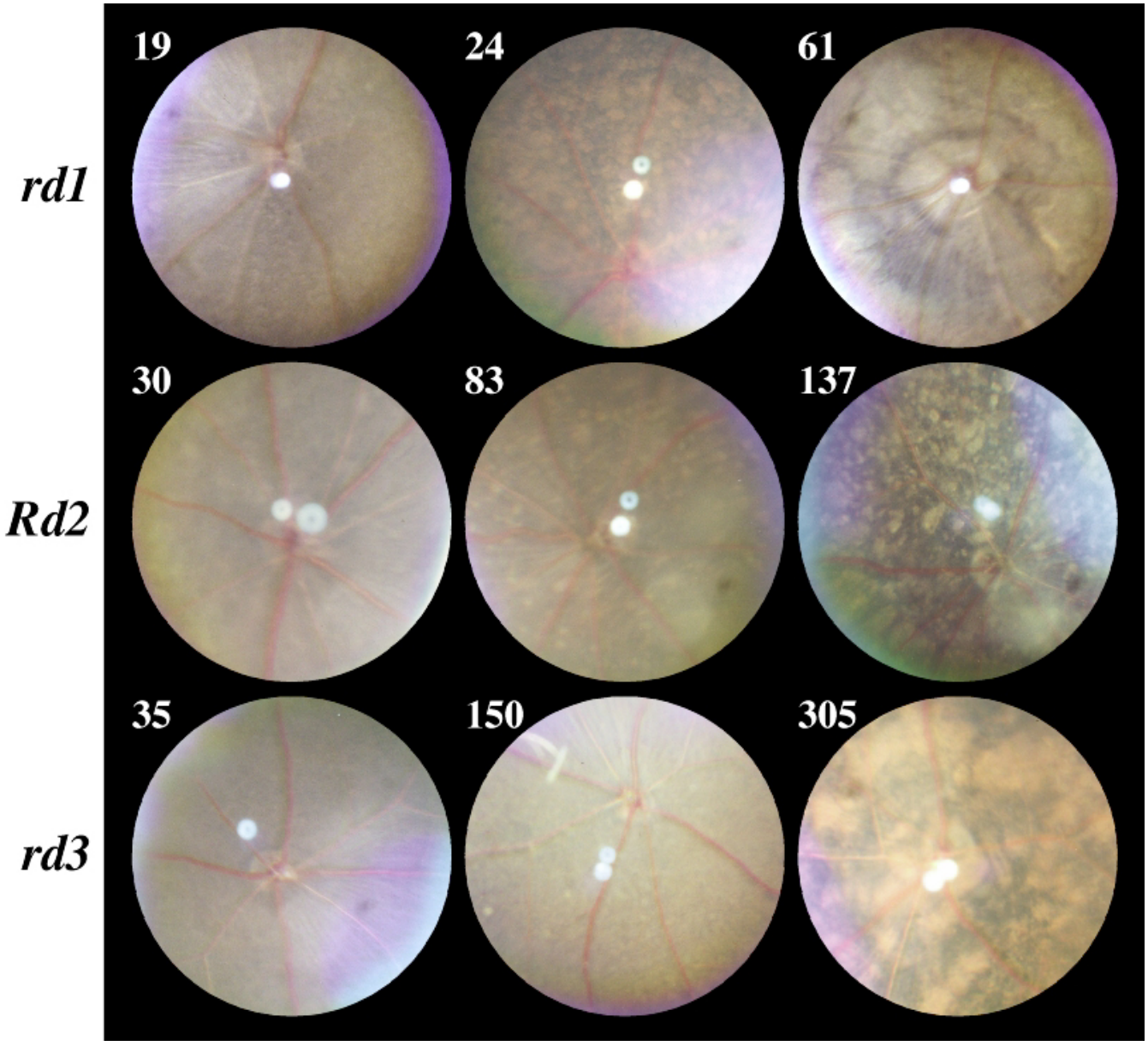

Figure 3. Progressive retinal changes. Numbers represent age in days. **Top panel**: retinal degeneration 1 (*rd1*). At 19 days the retina is similar to the normal C57BL/6J (see Figure 2), but there is narrowing of the retinal arterioles. By 24 days there is further narrowing of retinal vessels. Focal patches of RPE depigmentation are easily identified. By 61 days, all retinal vessels are narrowed and there are map-like areas of hypo- and hyperpigmentation. **Middle panel**: retinal degeneration 2 (*Rd2*). Vascular narrowing is present by 30 days of age. Development of spots of retinal pigment epithelium (RPE) depigmentation occurs by day 83. By day 137 the retina has a spotted appearance caused by areas of hypo- and hyperpigmentation of the RPE. Additional vascular narrowing is present. **Bottom panel**: retinal degeneration 3 (*rd3*). At 35 days, only vascular narrowing is seen. The degeneration has progressed by 150 days and there are small inconspicuous hypopigmented spots. In older mice (305 days) the areas of hypo- and hyperpigmentation of the RPE are prominent. For larger versions of an individual image, go to http://www.molvis.org/molvis/v5p22.

should be given 20-30 min before photography. Some strains dilate more easily than others. Albino strains are more sensitive to dilation than pigmented strains. Photosensitivity and pupillary contraction that limited photography was prevalent in wild derived strains and infrequent in common laboratory strains.

Representative fundus photographs of pigmented (C57BL/6J) and albino (BALB/cByJ) mouse strains are presented in Figure 2a and Figure 2b. While the image quality is very high, the small size of the mouse pupil makes it difficult to photograph the peripheral fundus.

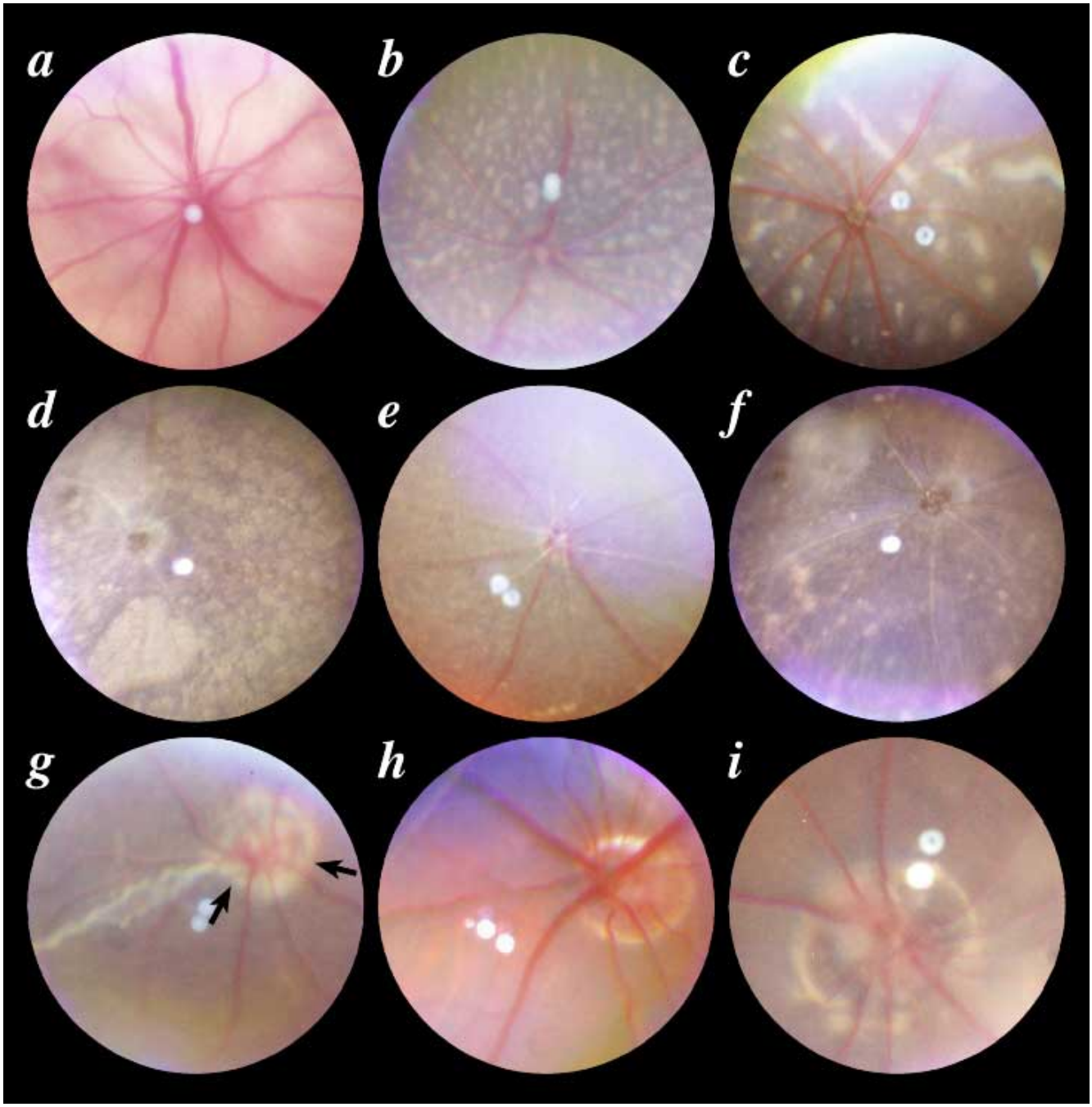

Figure 4. Catalogue of mutant phenotypes caused by the mouse mutations listed. Ages were typically selected to demonstrate well developed retinal changes. **A**: Achondroplasia (*cn*) at 6 weeks shows dilated venules. **B**: Typical retinal degeneration 7 (*rd7*) 3 weeks of age demonstrates a pattern of small white spots. **C**: In atypical *rd7* at 4 weeks of age, spots are larger, often elongated and fewer in number. **D**: Nervous (*nr*) 27 weeks of age shows larger spots that are forming confluent plaques of RPE hypopigmentation. All retinal vessels show severe narrowing. **E**: Motor neuron degeneration (*mnd*), 12 weeks of age, demonstrates retinal arteriole narrowing on a background of faintly hypopigmented spots. **F**: Purkinje cell degeneration (*pcd*), 45 weeks of age, also has severe narrowing of all retinal vessels. Hypopigmented spots of variable size and irregular arrangement are evident. **G**: Kidney and retinal defects (*Krd*),12 weeks of age, shows a large coloboma of the optic nerve (arrows) and a sectoral chorioretinal coloboma. **H**: Mice with the optic nerve coloboma phenotype (ONC), four weeks of age demonstrates a large coloboma of the optic nerve. **I**: CALB/Rk, 19 weeks of age, has a large optic nerve coloboma that appears to include peripapillary retina. For larger versions of an individual image, go to the web site, http://www.molvis.org/molvis/v5p22.

The general utility and reliability of this procedure is illustrated by documentation of progressive changes in various retinal degenerations over different time frames (Figure 3) and the cataloging of the fundus phenotypes in a number of mouse mutants (Figure 4). Clinical descriptions and histologic but not clinical images were previously published for the mutants *rd1, Rd2* and *rd3* [12-15].

The three progressive retinal degenerations that we analyzed are illustrated in Figure 3. Retinal degeneration-1 (*Pdeb*^{rd1}) demonstrates retinal changes of vascular sclerosis as early as 19 days of age. By 24 days, there are focal areas of retinal pigment epithelial depigmentation that are typical signs of retinal degeneration and that continue to progress. In retinal degeneration 2 (*Prph2*^{Rd2}) mice, vascular narrowing may be seen by 30 days and hypopigmented spots appear around 80 days of age. More advanced changes may not develop until five months of age. Retinal degeneration 3 (*rd3*) is the slowest of the described retinal degenerations to develop. In the genetic background studied here, vascular narrowing appears at 35 days. Hypopigmented spots appear at 5 months, but prominent retinal changes do not appear until 8 to 10 months of age.

Figure 4 illustrates the fundus appearance caused by a variety of mutations. Achondroplasia (*cn*) is a mutation reported to cause skeletal abnormalities while the ears and tail are markedly cyanotic [12, 16]. We found that the retinal veins are prominently dilated (compare to Figure 2) in these albino mice (Figure 4a). This strain is short-lived and we have observed no retinal degeneration.

Retinal degeneration 7 (*rd7*) (Figure 4b) is a recently discovered retinal degeneration [17]. At weaning age, the entire retina is covered by small spots. Sometimes young *rd7/rd7* mice have larger retinal dots as well as long retinal folds (Figure 4c). The retinal spots begin to disappear around 5 months of age. Electroretinogram amplitude is attenuated but stable until about 1 year when progressive loss of a and b wave amplitude begins [17].

Mice with the nervous mutation (*nr*) develop a severe Purkinje cell degeneration and have been reported to develop retinal degeneration that progresses slowly over the first year of life [14, 16, 18, 19]. By 27 weeks (Figure 4d), there are large areas of retinal degeneration and plaques of retinal pigment epithelial hypopigmentation.

Motor neuron degeneration (*mnd*) is an autosomal recessive mutation that causes hind limb paralysis and retinal degeneration [14, 16]. We have found that affected mice develop a granular appearance to the retina by six weeks and obvious retinal degeneration appears by 12 weeks (Figure 4e).

Mice with Purkinje cell degeneration (*pcd*) develop retinal degeneration involving the photoreceptors [14, 20, 21]. We have observed that this degeneration progresses slowly to its most severe state over the first year after birth. Hypopigmented spots and arteriolar narrowing are prominent features (Figure 4f).

The kidney and retinal defects mutation (*Krd*) [22] causes congenital colobomas (Figure 4g) as well as abnormal vasculature. There is considerable phenotypic variability with some eyes only having optic nerve involvement while others have colobomas of both the optic nerve and retina.

The ONC and CALB/Rk (CALB) strains have previously unreported developmental phenotypes. In mice with ONC, a large coloboma is present at birth and does not change with age (Figure 4h). CALB mice have an exceptionally large optic nerve coloboma (Figure 4i). Histologic analyses support the diagnosis of optic nerve coloboma in these strains. Experiments to map the genes responsible for the ONC and CALB phenotypes have not yet implicated any chromosomal regions. Many offspring in the mapping backcrosses had no obvious or only relatively mild abnormalities. Very few mice had the prominent colobomas similar to those of the parental ONC and CALB strains. The segregation pattern of phenotypic presence and severity suggests that multiple genes contribute to each phenotype. F1 offspring from crosses between ONC and CALB typically have prominent colobomas, suggesting that some of the same genes are involved in both strains.

Figure 5 presents examples of fluorescein angiography. We have found that intraperitoneal administration of fluorescein is adequate for fluorescein angiography in all mouse strains evaluated. Penetration through the omental and peritoneal vasculature is sufficiently rapid that an arterial-venous cycle can be observed. The retinal capillaries are clearly visualized (Figure 5a). Vascular leakage can be detected as pro-

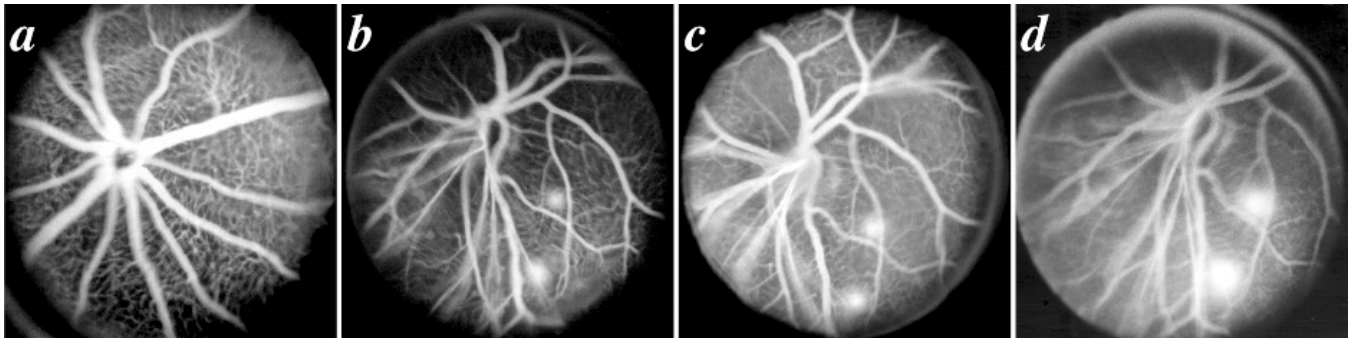

Figure 5. Fluorescein angiograms. **A**: Normal C57BL/6J mouse eight weeks of age, taken in early venous phase. All retinal arterioles and venules are filled with dye and details of the retinal capillary bed are easily visualized. **B-D**: Eight week old *Onc1* mouse, demonstrating an abnormal blood vessel pattern and two areas of inferolateral fluorescein leakage that become more apparent from early to late venous stages. The angiograms in Figures 5b-d were taken 143, 183, and 209 s after fluorescein administration. For larger versions of an individual image, go to the web site, http://www.molvis.org/molvis/v5p22.

gressively documented in another new mutation, *Onc1*that also causes optic nerve coloboma (Figure 5b-d).

DISCUSSION

Mice have an increasingly important role in ocular research. Clinical fundus examination and fundus photography are important tools to monitor and document the progression of ocular diseases. We have developed a reliable procedure that produces high quality images of the mouse fundus and permits recording of progressive retinal changes over time in the same animal. Additionally, fundus photography allows comparison of the phenotypes of newly discovered retinal mutants to existing mutants at other institutions and to potentially similar human conditions.

Mice present unique optical and photographic challenges due to their small eye size (diameter of 3 mm) and the small radius of curvature of the cornea and lens. Although it is possible to view the peripheral retina with an indirect ophthalmoscope (with some distortion), peripheral retinal photography is very difficult and we have not produced high quality photographs. Even in the posterior fundus, depth of focus is limited because of the steep radius of curvature of the eye. Multiple exposures can be used to achieve sharp images of both retinal details and the retinal vessels. Nevertheless, in most cases focusing to have both retina and retinal vessels in reasonable focus captured satisfactory detail. An advantage of the method for fundus photography described here is that with gentle but secure restraint, one can photograph unanesthetized conscious mice. If necessary, it is also possible to use anesthetized or sedated mice but care must be taken to avoid ocular clouding.

We present clinical photographs and in some cases photodocumentation of disease progression for a number of commonly analyzed mouse mutations, including *Pdeb*^{rd1}, *Prph2*^{Rd2}, and *rd3*. These images have been lacking in the literature and will facilitate understanding and comparison of the disease phenotypes. In addition, we document unreported ocular phenotypes in *cn*/*cn*, CALB/Rk, ONC and *Onc1* mice. CALB/Rk and ONC have colobomas of the optic nerve and retina similar to human cavitary defects of the optic nerve [23, 24]. The CALB/Rk phenotype in some ways resembles the human morning glory syndrome [25].

Care must be taken when comparing our clinical findings to previous histologic reports. This is for a number of reasons including the amount of pathologic detail provided, differences in genetic background, possible environmental differences that may affect progression, and the fact that degenerative changes are sometimes described to exist by a specific age but the first age at which they appear may not be clear as it was not feasible to study all earlier ages. Within these constraints, comparison of our clinical findings to previous histologic reports for *rd1* and *Rd2* indicates that the relative rate of clinical progression for *rd1* and *Rd2* appears to correlate well with the progression of histologic changes. Although we have not conducted detailed comparisons of clinical and histologic progression for these diseases, our experience suggests that clinically obvious changes such as RPE depigmentation tend to lag behind photoreceptor loss. In the case of *rd3,* this seems to be particularly evident. The rd3 phenotype is known to be significantly altered by genetic background [15] and so we will only discuss the In(5)30Rk background here. Histologically, disorganization and severe loss of photoreceptors has been reported to occur over the first 16 weeks of age and decreasing ERG amplitude and photoreceptor loss correlated well [15]. In the current clinical study, vascular narrowing was present at 35 days but hypopigmented spots were not observed until 5 months and severe global RPE depigmentation was not present until 10 months of age. Although, vascular changes can be a sensitive indicator of retinal disease, great care must be taken to ensure that they are real and not a consequence of artifactually reduced blood flow. Changes in retinal thickness are difficult to detect clinically. Other than vascular narrowing and sclerosis, the mouse fundus can appear relatively normal (though granular) even at stages when only 2 or 3 layers of photoreceptor nuclei remain. In general, RPE depigmentation lags behind photoreceptor loss and that is why obvious clinical fundal depigmentation lags behind histologically detectable decreases in photoreceptor number. Thus, even though clinical fundus examination provides an inexpensive and rapid method to screen for retinal disease and is the method we most often use for initial strain analysis, ERG evaluation is very sensitive to photoreceptor loss and recommended for more sensitive early detection of photoreceptor abnormalities.

Intraperitoneal fluorescein injection is successfully used in producing fluorescein angiograms that demonstrate the normal arterial-venous dye cycle. Subtle retinal vascular abnormalities, retinal capillary angiopathy and vascular leakage can only be seen using this technique. We now routinely use angiography in the characterization of newly discovered eye mutants. Dye leakage has been demonstrated in several mutant mouse strains in which there would otherwise have been no reason to suspect the presence of abnormal vessels. Similarly, fluorescein angiography revealed previously unsuspected vascular leakage in *Onc1* mice that had apparently intact vessels on routine ophthalmoscopic examination. Angiography in conscious mice also may allow demonstration of altered blood flow and filling defects, and demonstration of small vitreous vessels. Angiography is simpler than fundus photography because there is no reflection from an illumination lamp and focusing on retinal vessels is straightforward. The technique has not been successful in albino mice because the absence of pigment in the retinal pigment epithelium and choroid results in severe glare.

In summary, we have developed a reliable method for photodocumentation of fundus lesions and for retinal angiography in conscious mice. As we demonstrate here, these methods will be important for documenting disease findings and progression in mice with newly induced or spontaneous mutations. The cost of the photography system is not overly prohibitive for many laboratories (currently <$15,000) and any person with good mouse handling skills should be able to produce quality images.

ACKNOWLEDGEMENTS

We thank William Bromley, M.D. for the loan of the RC-2

fundus camera, Jennifer Smith for assistance with the figures, Felicia Farley for help with references, and Michael Anderson, Patsy Nishina, and John Schimenti for critical reading of the manuscript. Supported in part by grants EY07758, CA34196, AHAF G1999023, and a grant from The Foundation Fighting Blindness. SWMJ is an Assistant Investigator of The Howard Hughes Medical Institute. Proprietary interest: none.

REFERENCES

1. Zack DJ. Of mice and men: what mice can teach us about human ophthalmic disease. Arch Ophthalmol 1993; 111:911-3.
2. Paigen K. A miracle enough: the power of mice. Nat Med 1995; 1:215-20.
3. Smithies O, Maeda N. Gene targeting approaches to complex genetic diseases: atherosclerosis and essential hypertension. Proc Natl Acad Sci U S A 1995; 92:5266-72.
4. Schimenti J, Bucan M. Functional genomics in the mouse: phenotype-based mutagenesis screens. Genome Res 1998; 8:698-710.
5. John SWM, Anderson MG, Smith RS. Mouse genetics: a tool to help unlock the mechanisms of glaucoma. J Glaucoma. In press 1999.
6. Winston JV, Heckenlively JR, Roderick TH. Screening for mouse retinal degenerations. II. Molossinus MOLC and MOLD strains. Doc Ophthalmol 1989; 71:241-52.
7. DiLoreto D Jr, Grover DA, del Cerro C, del Cerro M. A new procedure for fundus photography and fluorescein angiography in small laboratory animal eyes. Curr Eye Res 1994; 13:157-61.
8. Nakamura A, Yokoyama T, Kodera S, Zhang D, Hirose S, Shirai T, Kanai A. Ocular fundus lesions in systemic lupus erythematosus model mice. Jpn J Ophthalmol 1998; 42:345-51.
9. Olsson JE, Gordon JW, Pawlyk BS, Roof D, Hayes A, Molday RS, Mukai S, Cowley GS, Berson EL, Dryja TP. Transgenic mice with a rhodopsin mutation (Pro23His): a mouse model of autosomal dominant retinitis pigmentosa. Neuron 1992; 9:815-30.
10. Ikeda S, Hawes NL, Chang B, Avery CS, Smith RS, Nishina PM. Severe ocular abnormalities in C57BL/6 but not in 129/Sv p53-deficient mice. Invest Ophthalmol Vis Sci 1999; 40:1874-8.
11. Okamoto N, Tobe T, Hackett SF, Ozaki H, Vinores MA, LaRochelle W, Zack DJ, Campochiaro PA. Transgenic mice with increased expression of vascular endothelial growth factor in the retina: a new model of intraretinal and subretinal neovascularization. Am J Pathol 1997; 151:281-91.
12. Doolittle DP, Davisson MT, Guidi JN, Green MC. Catalog of mutant genes and polymorphic loci. In: Lyon MF, Rastan S, Brown SDM, editors. Genetic variants and strains of the laboratory mouse. 3rd ed. Oxford. Oxford University Press; 1996. p. 17-854.
13. Chang B, Heckenlively JR, Hawes NL, Roderick TH. New mouse primary retinal degeneration (rd-3). Genomics 1993; 16:45-9.
14. Roderick TH, Chang B, Hawes NL, Heckenlively JR. New retinal degenerations in the mouse. In: Anderson RE, LaVail MM, Hollyfield JG, editors. Degenerative diseases of the retina. New York: Plenum Press; 1995. p. 77-85.
15. Heckenlively JR, Chang B, Peng C, Hawes NL, Roderick TH. Variable expressivity of rd-3 retinal degeneration dependent on background strain. In: Hollyfield JG, Anderson RE, LaVail MM, editors. Retinal degeneration: clinical and laboratory applications. New York: Plenum Press; 1993. p. 273-80.
16. Mouse Genome Database (MGD), Mouse Genome Informatics Project. The Jackson Laboratory, Bar Harbor, ME. July 1999. Available from: The Jackson Laboratory Mouse Genome Informatics (MGI) Homepage, http://www.informatics.jax.org.
17. Chang B, Heckenlively JR, Hawes NL, Davisson MT. A new mouse model of retinal dysplasia and degeneration (rd7). Invest Ophthalmol Vis Sci 1998; 39:S880.
18. Mullen RJ, LaVail M. Two types of retinal degeneration in cerebellar mutant mice. Nature 1975; 258:528-30.
19. White MP, Gorrin GM, Mullen RJ, LaVail MM. Retinal degeneration in the nervous mutant mouse. II. Electron microscopic analysis. J Comp Neurol 1993; 333:182-98.
20. Blanks JC, Mullen RJ, LaVail MM. Retinal degeneration in the pcd cerebellar mutant mouse. II. Electron microscopic analysis. J Comp Neurol 1982; 212:231-46.
21. LaVail MM, Blanks JC, Mullen RJ. Retinal degeneration in the pcd cerebellar mutant mouse. I. Light microscopic and autoradiographic analysis. J Comp Neurol 1982; 212:217-30.
22. Keller SA, Jones JM, Boyle A, Barrow LL, Killen PD, Green DG, Kapousta NV, Hitchcock PF, Swank RT, Meisler MH. Kidney and retinal defects (Krd), a transgene-induced mutation with a deletion of mouse chromosome 19 that includes the Pax2 locus. Genomics 1994; 23:309-20.
23. Pagon RA. Ocular coloboma. Surv Ophthalmol 1981; 25:223-36.
24. Slusher MM, Weaver RG Jr, Greven CM, Mundorf TK, Cashwell LF. The spectrum of cavitary optic disc anomalies in a family. Ophthalmology 1989; 96:342-7.
25. Sobol WM, Bratton AR, Rivers MB, Weingeist TA. Morning glory disk syndrome associated with subretinal neovascular membrane formation. Am J Ophthalmol 1990; 110:93-4.
26. Hopp RM, Ransom N, Hilsenbeck SG, Papermaster DS, Windle JJ. Apoptosis in the murine rd1 retinal degeneration is predominantly p53-independent. Mol Vis 1998; 4:5 .
27. Sanyal S, De Ruiter A, Hawkins RK. Development and degeneration of retina in rds mutant mice: light microscopy. J Comp Neurol 1980; 194:193-207.